



# Oxygen-induced retinopathy in the mouse.

## Citation

Smith, Lois E. H., Wesolowski, Eva, McLellan, Angela, Sandra K. Kostyk, Robert D'Amato; Richard Sullivan; Patricia A. D'Amore. 1994. Oxygen-induced retinopathy in the mouse. *Investigative Ophthalmology & Visual Science* 35(1):101-11

## Permanent link

<http://nrs.harvard.edu/urn-3:HUL.InstRepos:36304244>

## Terms of Use

This article was downloaded from Harvard University's DASH repository, and is made available under the terms and conditions applicable to Other Posted Material, as set forth at <http://nrs.harvard.edu/urn-3:HUL.InstRepos:dash.current.terms-of-use#LAA>

## Share Your Story

The Harvard community has made this article openly available.  
Please share how this access benefits you. [Submit a story](#).

[Accessibility](#)

# Oxygen-Induced Retinopathy in the Mouse

Lois E. H. Smith,\* Eva Wesolowski,\* Angela McLellan,\* Sandra K. Kostyk,†  
Robert D'Amato,\* Richard Sullivan,\* and Patricia A. D'Amore†‡

**Purpose.** To develop oxygen-induced retinopathy in the mouse with reproducible and quantifiable proliferative retinal neovascularization suitable for examining pathogenesis and therapeutic intervention for retinal neovascularization in retinopathy of prematurity (ROP) and other vasculopathologies.

**Methods.** One-week-old C57BL/6J mice were exposed to 75% oxygen for 5 days and then to room air. A novel fluorescein-dextran perfusion method has been developed to assess the vascular pattern. The proliferative neovascular response was quantified by counting the nuclei of new vessels extending from the retina into the vitreous in 6  $\mu$ m sagittal cross-sections. Cross-sections were also stained for glial fibrillary acidic protein (GFAP).

**Results.** Fluorescein-dextran angiography delineated the entire vascular pattern, including neovascular tufts in flat-mounted retinas. Hyperoxia-induced neovascularization occurred at the junction between the vascularized and avascular retina in the mid-periphery. Retinal neovascularization occurred in all the pups between postnatal day 17 and postnatal day 21. There was a mean of 89 neovascular nuclei per cross-section of 9 eyes in hyperoxia compared to less than 1 nucleus per cross-section of 8 eyes in the normoxia control ( $P < 0.0001$ ). Proliferative vessels were not associated with GFAP-positive astrocyte processes.

**Conclusions.** The authors have described a reproducible and quantifiable mouse model of oxygen-induced retinal neovascularization that should prove useful for the study of pathogenesis of retinal neovascularization as well as for the study of medical intervention for ROP and other retinal angiopathies. Invest Ophthalmol Vis Sci. 1994;35:101-111

Exposure of premature infants to hyperoxia or to the relative hyperoxia of the nonuterine environment is associated with retinopathy. This retinopathy of prematurity (ROP) usually regresses but can lead to irreversible vision loss if there is progression from retinal neovascularization to cicatrization and retinal detachment. In previous attempts to develop a mouse model of oxygen-induced retinopathy, the neovascular response to hyperoxia has been inconsistent and unquantified.<sup>1-9</sup>

We have defined parameters for exposure to hyperoxia that produce consistent, reproducible neovas-

cularization in the mouse retina. Two new methods have been developed to assess and quantify the vascular response. This reproducible, quantifiable, and inexpensive model reflects retinal neovascularization in general and the proliferative neovascular phase of ROP in particular. It should prove effective for testing medical intervention and for elucidating the pathophysiology of proliferative retinopathy.

## METHODS

### Animal Model

This study adhered to the ARVO Statement for the Use of Animals in Ophthalmic and Vision Research. Neonatal mice (C57BL/6J) were obtained from breeding colonies maintained at the Children's Hospital in Boston, Massachusetts. To develop the model, we examined retinopathy as a function of age at initial exposure to hyperoxia and of oxygen concentration. Initially, mice from birth (P0) to postnatal day 7 (P7) were exposed to 5 days of hyperoxia, and their eyes were examined by histologic cross-section after 1 to 5

From the Departments of \*Ophthalmology, †Pathology, and ‡Surgical Research, Harvard Medical School and The Children's Hospital, Boston, Massachusetts. Supported in part by Lions Foundation Inc. of Massachusetts; National Institutes of Health grants EY08670 (LEHS), EY05318 (PAD), and EY00311 (SKK); and by Knights Templar Eye Foundation Inc. and Fight for Sight/National Society to Prevent Blindness grants (EW). Submitted for publication March 3, 1993; revised May 25, 1993; accepted June 17, 1993.

Proprietary interest category: N.

Reprint requests: Lois E. H. Smith, MD, PhD, Department of Ophthalmology, The Children's Hospital, 300 Longwood Avenue, Boston, MA 02115.

days in room air. Mice were chosen at P7 to optimize the balance in retinal development between hyaloid regression and incomplete retinal vascularization.<sup>9</sup> Litters of P7 pups with at least two nursing dams per group were assigned to hyperoxia (75% oxygen) or to room air. Seventy-five percent oxygen was chosen after examining the effect of 50% to 95% oxygen on neovascularization. The mice were exposed to less than 300 lux of 12-hour cyclical broad spectrum light. Surrogate dams were substituted if nursing dams died, a rare occurrence. The oxygen-treated mice were housed in an incubator connected to a Bird 3-M oxygen blender (Palm Springs, CA) with oxygen and nitrogen, allowing adjustment of oxygen concentration to  $75\% \pm 2\%$ . A flow rate of 1.5 l/min was checked twice daily. Oxygen concentration was monitored with a Beckman oxygen analyzer (Model D2, Irvine, CA). The cage temperature was maintained at  $23^{\circ}\text{C} \pm 2^{\circ}\text{C}$ . The mice were placed in the oxygen chamber with enough food and water to sustain them for 5 days. The chamber was not opened during hyperoxia exposure from P7 to P12. On P12, the animals were returned to room air until P17 to P21, when the retinas were assessed for maximum neovascular response. The animals were weighed before and after oxygen exposure. Animals not sacrificed by P21 were assessed from P21 to P44 for regression of neovascularization and normalization of the vascular pattern. To establish the preferential susceptibility of immature versus adult vasculature to hyperoxia, we exposed P24 mice with fully developed retinal vasculature to hyperoxia for 5 days, then to room air, and assessed the retinal vascular pattern for vaso-oblivation and neovascularization. The eyes were processed as described below.

### Angiography Using High Molecular Weight Fluorescein-Dextran

Mice were deeply anesthetized intraperitoneally with tribromoethanol (0.2 ml/10 g body weight) and then perfused through the left ventricle with 1 ml of phosphate buffered saline (PBS) containing 50 mg of  $2 \times 10^6$  molecular weight fluorescein-dextran (Sigma, St. Louis, MO). (Lower molecular weight dextrans were found to leak from the vessels during fixation.)<sup>10</sup> Before use, the fluorescein-dextran solution was clarified by centrifugation for 5 minutes at 10,000 rpm (Fisher Scientific, Springfield, NJ, model 235 C). The eyes were marked for orientation, enucleated, and placed in 4% paraformaldehyde for 3 to 24 hours. Lenses were removed and peripheral retinas were cut to allow flat-mounting with glycerol-gelatin. The flat-mounted retinas were viewed by fluorescence microscopy (Zeiss Axiophot, Thornwood, NY) and photographed.

### Staining With RCA Lectin

To be certain that neovascular tufts were delineated by the fluorescein-dextran perfusion method, some of

the fluorescein-dextran perfused retinas were also stained with RCA-I lectin, which labels mouse retinal vasculature.<sup>11,12</sup> The retinas were processed as previously described<sup>13</sup> and flat-mounted with glycerol-gelatin for viewing by fluorescence microscopy.

### Quantification of Neovascular Proliferative Retinopathy

At P21, mice were sacrificed with intraperitoneal tribromoethanol (0.1 ml/g body weight). The eyes were enucleated, immersed in 4% paraformaldehyde in PBS for at least 24 hours, and embedded in paraffin. Serial sections (6  $\mu\text{m}$ ) of whole eyes were cut sagittally, through the cornea and parallel to the optic nerve and stained with periodic acid-Schiff (PAS) and hematoxylin. For this study, eyes were not oriented as to nasal and temporal sections because preliminary data revealed no difference in neovascularization in any quadrant of oriented cross-sections and flat-mounts. Nuclei from new vessels and vessel profiles could be distinguished from other structures in the retina and counted in cross-section with light microscopy (magnification  $\times 400$ ).

Approximately 150 serial sections were cut from each eye. In the central half of the globe, between two and four sections on each side of the optic nerve, 30 to 90  $\mu\text{m}$  apart, were counted for neovascularization. This sampling method yielded between four and eight sections per eye that were within 10% of the mean retinal length. Cross-sections that included the optic nerve were excluded because normal vessels emanating from the optic nerve, though distinguishable from the neovascularization extending into the vitreous, fulfilled the counting criterion and would have increased the error. Vascular cell nuclei, identified under light microscopy with hematoxylin staining, were considered to be associated with new vessels if they were found on the vitreal side of the internal limiting membrane. Pericytes were not morphologically identified in the neovascular tufts and have not been reported to be associated with neovascular vessels. Nonetheless, it is possible that pericytes or pericyte precursors may have been included in our cell counts. Intraretinal vessels were distinguished from neural retina with PAS staining. The unpaired two-tailed Student's *t*-test was used to compare the number of neovascular nuclei and to compare the number of intraretinal vascular profiles in the mice exposed to hyperoxia or normoxia.

### GFAP Immunolocalization

Mice were anesthetized with tribromoethanol and then perfused through the left ventricle with 4% paraformaldehyde in 0.1 sodium phosphate buffer, pH 7.4. Corneas were removed and the eyes were post-fixed for 30 minutes, rinsed in 0.1 M  $\text{NaH}_2\text{PO}_4$ , pH

7.4, and equilibrated in 30% sucrose overnight at 4°C. Eyes were embedded in Tissue-tek (Miles Inc., Elkhart, IN), frozen, and stored at -80°C. Tissue sections of 10 to 12  $\mu$ m were cut onto glass slides in a cryostat at -22°C and were successively incubated as follows: 10% normal goat serum (NGS; Sigma) for 30 minutes at room temperature; rabbit anti-bovine GFAP (Incstar Corp., MI) at 1:1200 in 1% NGS, 0.3% Triton-X 100, overnight at 4°C; secondary antiserum (biotinylated goat anti-rabbit) (Vector Labs, Burlingame, CA) in 1% NGS, 0.3% Triton-X 100 for 1 hour at room temperature; avidin-biotin complex (Vector Labs) for 1 hour at room temperature; 0.05% diaminobenzidine (Sigma) in 0.01% hydrogen peroxide, 50 mM Tris-HCl for 1 to 3 minutes at room temperature. The incubations included appropriate washings with PBS between steps. Coverslips were applied, and slides were then examined by light microscopy.

## RESULTS

### Development of Animal Model

Observation of hyaloid regression and retinal vascular formation in the mouse from P0 to P7 revealed that the vascular development of P7 retinas most closely resembled that of premature infants with optimization of maximal hyaloid vascular regression and minimal retinal vascular development. P0 mice (with less regressed hyaloid vessels), when exposed to greater than 80% oxygen from birth, had extensive dilatation of the hyaloid vessels and extensive neovascularization at the disk that was neither quantifiable nor reproducible (data not shown). In contrast, exposure of P7 mice to 5 days of 75% oxygen followed by return to room air resulted in reproducible and quantifiable retinal neovascularization without hypertrophy or dilatation of the hyaloid vessels. P7 mice exposed to greater than 80% oxygen had slightly more retinal neovascularization but a much higher mortality rate due, at least in part, to a much higher maternal mortality rate. We therefore did not use greater than 80% oxygen but used 75% oxygen where mortality was low.

Mice were examined daily after removal from hyperoxia to room air on P12 to P44 to find the day at which induced neovascularization was maximal. The greatest neovascular response occurred from P17 to P21; it was followed by slow regression of the new vessels with reestablishment of a more normal branching vascular pattern, visible in retinal flat-mounts by P24. Exposure of P24 mice with an adult retinal vascular pattern to 5 days of 75% oxygen followed by room air did not result in hypoperfusion or retinal neovascularization.

### Hyperoxia-Induced Proliferative Retinopathy

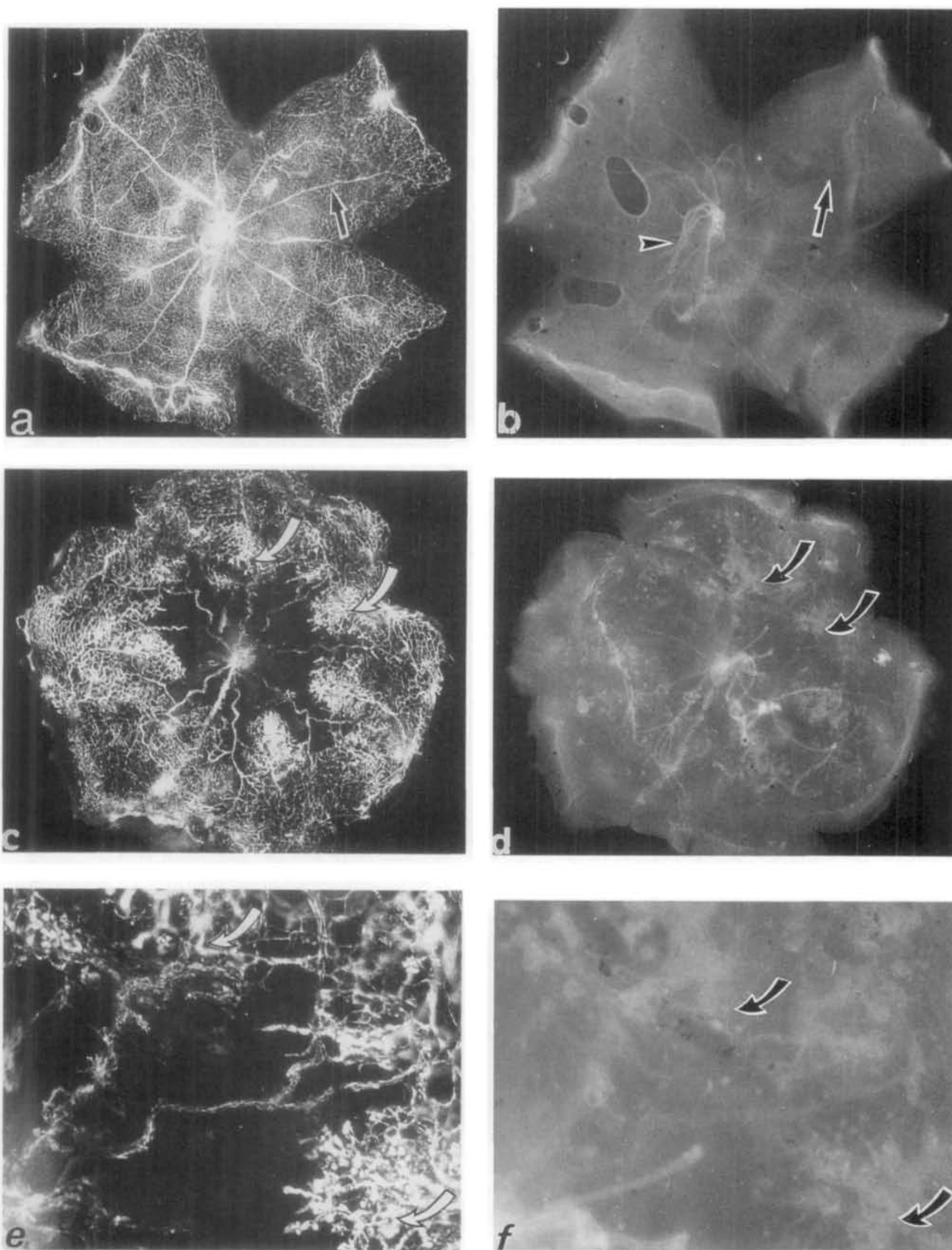
The pattern of vascular development and neovascularization was seen readily in retinal flat-mounts after fluo-

orescein-dextran perfusion.<sup>13</sup> In earlier studies, we used India ink to visualize the total retinal vascular pattern and observed patchy perfusion of the capillaries with little or no delineation of the neovascular tufts extending into the vitreous. Vessels were more completely delineated with fluorescein-dextran than with India ink, and retinas had minimum background staining. By focusing through the tissue, the deep and superficial vascular plexuses were distinguishable and neovascular tufts were visible. The labeled vessels were stable for at least 10 months without additional diffusion or decay of label.

The retina of the normal P17 mouse had both superficial and deep vascular layers (joined by connecting vessels) that extended from the optic nerve to the periphery. The vessels formed a fine radial branching pattern in the superficial retinal layer and a polygonal reticular pattern in the deep retinal layer (Fig. 1a). The retinal vascular pattern in the mice exposed to hyperoxia was characterized by decreased central perfusion in both the superficial and the deep layers (Fig. 1c). The neovascular response, as in humans, occurred in mid-periphery at the junction between the perfused and the nonperfused retina. Unlike ROP in humans, however, the nonperfused retina was central and the perfused retina was peripheral. Remnants of hyaloid vessels maintained interconnection with peripheral retinal vessels (seen in paraffin cross-section; data not shown). This pattern was present in all mice (21 retinas at P17 and 32 retinas at P21) exposed to hyperoxia. In both fluorescein-dextran perfused flat-mounts and paraffin cross-sections, there was no correlation between the degree of hyperoxia-induced vasoproliferation and the sex or weight of the mouse pups.

To determine if fluorescein-dextran perfusion reveals all the neovascular tufts, several retinas that had been perfused with fluorescein-dextran were also exposed to Texas Red-labeled RCA-I lectin that binds selectively to murine vessels.<sup>11,12</sup> The RCA-I lectin labeled the vessels on the retinal surface and those extending into the vitreous of the normal and hyperoxia-exposed mice as well as the regressing hyaloid system (Figs. 1b, 1d). Consistent with the fluorescein-dextran perfusion pattern, the Texas Red-labeled RCA-I lectin highlighted the superficial radial vessels in both the normal mice and those exposed to hyperoxia, as well as the neovascular tufts in the hyperoxia-exposed mice. There were few, if any, new retinal vessels revealed with RCA-lectin staining (Figs. 1d, 1f) that were not also delineated by fluorescein-dextran perfusion (Figs. 1c, 1e). A few linear strands emanating from the disc did not perfuse with fluorescein-dextran yet were labeled with RCA lectin. These were likely to be remnants of regressing hyaloid vessels that no longer had patent lumina.

Examination of 6  $\mu$ m paraffin-processed cross-sections of normal and hyperoxia-treated mouse eyes



confirmed aspects of the vascular pattern seen with fluorescein-dextran angiography and added complementary details. The normal pattern, at P21, consisted of branching superficial vessels connecting with a deep vascular layer that extended from the optic nerve to the ora serrata. Vascular cells, defined by PAS and hematoxylin staining, did not extend beyond the internal limiting membrane into the vitreous (Fig. 2a). Mice exposed to hyperoxia from P7 to P12 and returned to room air until P21 had neovascular tufts, particularly in the mid-periphery, extending beyond the internal limiting membrane into the vitreous (Figs. 2b, 2c). The neovascular tufts visualized by perfusion with fluorescein-dextran (Figs. 1c, 1e) were found in some cross-sections to be contiguous with the deeper retinal vessels (Fig. 2c), confirming their origin from retinal rather than vitreal or hyaloid vessels. In cross-section, there was no difference in the morphology or thickness of the choroid between the areas of retinal hypoperfusion and perfusion (data not shown).

### Quantification of Proliferative Retinopathy

The degree of hyperoxia-induced neovascularization was quantified in serial paraffin cross-sections by counting the number of vascular cell nuclei on the vitreal side of the internal limiting membrane. In normal P21 mice, there was an average of  $0.6 \pm 0.9$  SD (SEM = 0.1) nuclei extending into the internal limiting membrane per 6  $\mu$ m retinal cross-section compared to  $89 \pm 34$  SD (SEM = 3) nuclei per 6  $\mu$ m cross-section in the hyperoxia-treated mouse eyes (Fig. 3). Although the profiles of the deeper vessels were no more numerous per 6  $\mu$ m cross-section in the hyperoxia-exposed retinas (Fig. 4), the average profile appeared greater in cross-sectional area (Fig. 2) and stained more heavily with PAS than did the vascular profiles in the normal retinas (data not shown). Further, the deeper vessels appeared to have more nuclei per profile area at P15 and P16 than did the normal retinas (data not shown). During the regressive phase (P21 to P44), the deeper vessels lost nuclei before PAS-stained material de-

creased, suggesting that extracellular material persisted longer than intracellular components during regression.

### Time Course of Hyperoxia-Induced Retinopathy

Other hyperoxia-induced changes were evident before the development of proliferative retinopathy. Normal P7 retinas had a superficial layer of vessels extending close to the ora serrata and a deeper connecting layer reaching from the optic nerve to the mid-periphery; there was also a small, nonperfused area at the ora serrata where vascular development had not yet occurred (Fig. 5a). After 8 hours of exposure to hyperoxia, there was decreased perfusion of the fine branching capillaries around the optic disc, presumably due to vasoconstriction, whereas the large, well-developed, superficial radial vessels extending from the optic disc were still perfused (Fig. 5b). This central vasoconstriction was reversible; mice removed from hyperoxia after 8 hours appeared to have normal retinal vascular patterns 5 days later. After 24 hours (Fig. 5c) and 5 days (Fig. 5d) of hyperoxia, the area of central hypoperfusion was progressively larger than it was with 8 hours of exposure (Fig. 5b). At P14, after 5 days of exposure to hyperoxia followed by 2 days in room air (Fig. 5e), most of the central retina showed almost no perfusion. The radial vessels appeared tortuous and dilated.

The reversibility of the hypoperfusion decreased after 24 hours of exposure to hyperoxia. Five days after removal to room air (P16), clusters of vascular cell nuclei were seen above the internal limiting membrane in paraffin cross-sections. Neovascular tufts extending into the vitreous occurred in the mid-periphery, at the junction of the central nonperfused retina and the peripheral well-perfused retina. This response was maximal between P17 and P21. Subretinal hemorrhages and retinal folds were seen in cross-sections of the hyperoxia-exposed retinas between P17 and P21, as have been described in oxygen-induced retinopathy

**FIGURE 1.** Comparison of fluorescein-dextran perfused and RCA lectin-labeled retinas exposed to room air or hyperoxia. (a) Fluorescein-dextran perfused retina from room air-raised P17 mouse. Arrow shows superficial radial vessel coincident with that seen in (b). This pattern was consistent in 16 mice over 8 experiments. (b) Same retina as in a, double-labeled with RCA-I lectin bound to Texas Red to delineate vessels on the retinal surface; *arrowhead* shows regressed hyaloid remnants; *arrow* shows superficial radial vessel. Note the absence of neovascular tufts. (c) Fluorescein-dextran perfused retina from P17 mouse exposed to hyperoxia from P7 to P12, before return to room air. Note area of central hypoperfusion. Arrows point to neovascular tufts extending into the vitreous. This pattern was consistent in 21 mice over 9 experiments. (d) Same retina as in c, double-labeled with RCA-I lectin bound to Texas Red. *Arrows* indicate neovascular tufts that coincide with perfused neovascular tufts in (c). (a to d) Original magnification  $\times 6$ . (e)  $25\times$  magnification of (c). *Arrows* indicate same vascular areas as indicated in c. (f)  $25\times$  magnification of areas indicated in d.

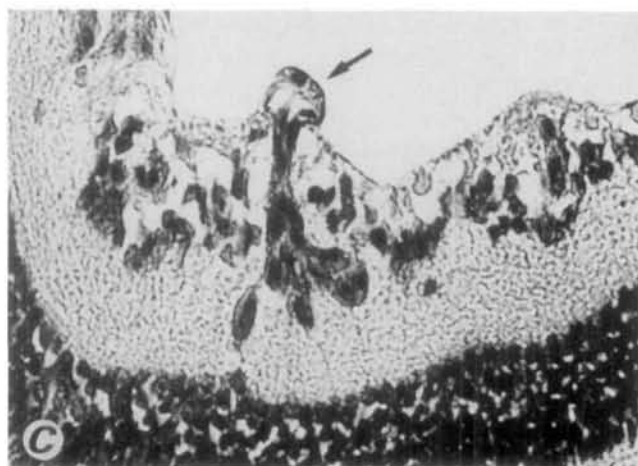
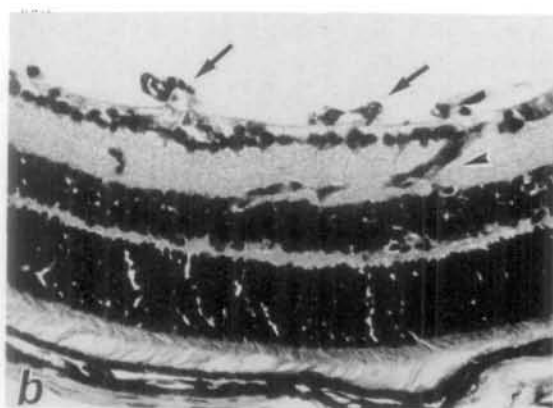
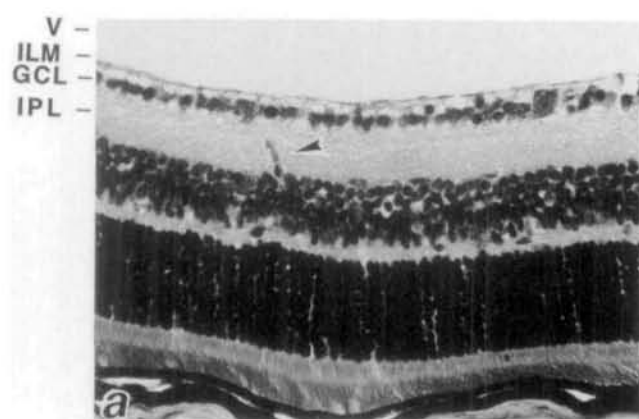


**FIGURE 2.** Comparison of room air and hyperoxia-exposed retinas in 6  $\mu$ m cross-section stained with PAS and hematoxylin. (a) P21 retina exposed to room air. Arrowhead indicates normal intraretinal vessel. (b) P21 retina exposed to hyperoxia from P7 to 12, before return to room air. Arrows indicate neovascular tufts extending into the vitreous. Arrowheads mark enlarged intraretinal vessel profiles. (a, b) Original magnification  $\times 100$ . (c) Higher magnification ( $\times 140$ ) of P17 retina exposed to hyperoxia from P7 to 12. Arrow indicates neovascular tuft extending into the vitreous, contiguous with a deeper intraretinal vessels. V, vitreous; ILM, internal limiting membrane; GCL, ganglion cell layer; IPL, inner plexiform layer.

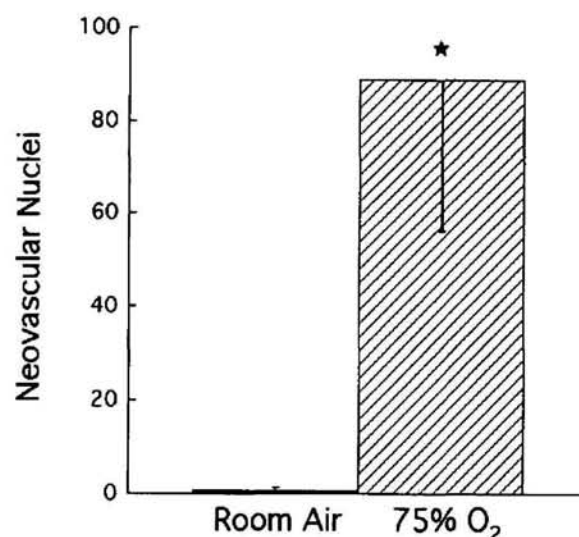


**FIGURE 3.** Quantification of proliferative neovascular response to hyperoxia. Total number of vascular nuclei per 6  $\mu$ m retinal cross-section, extending from the internal limiting membrane into the vitreous were counted; 9 eyes from 8 mice in 6 experiments (43 cross sections) in hyperoxia (89 nuclei; SD = 34; SEM = 3) were compared to 11 eyes from 9 mice (57 cross-sections) in 2 experiments in room air (0.6 nuclei; SD = 0.9; SEM = 0.1). Values in bar graph represent mean number nuclei  $\pm$  SD (\* $P < 0.0001$ ). See Figures 2a and 2b for comparison.

in other animals.<sup>1,14</sup> Mice with adult retinal vasculature (P24) exposed to 5 days of hyperoxia followed by a return to room air showed no hypoperfusion or proliferative retinopathy.

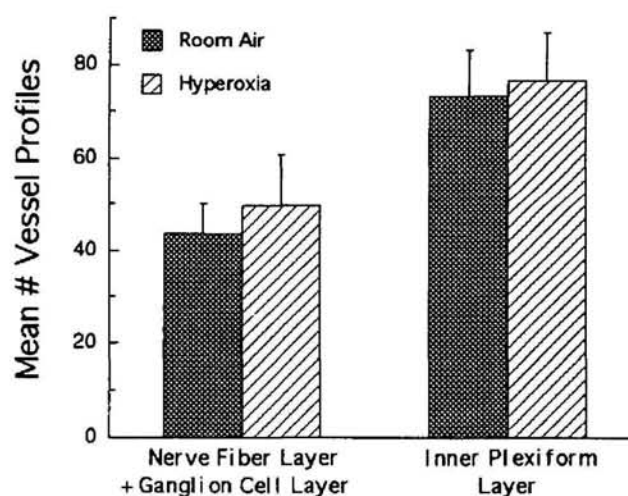


**FIGURE 4.** Intraretinal vascular response to hyperoxia. Vessel profiles in the ganglion cell layer and nerve fiber layer and in the inner plexiform layer were counted and expressed as mean number  $\pm$  SD per 6  $\mu$ m retinal cross-section ( $P > 0.05$  for room air versus hyperoxia). The same cross-sections as in Figure 2 were examined.



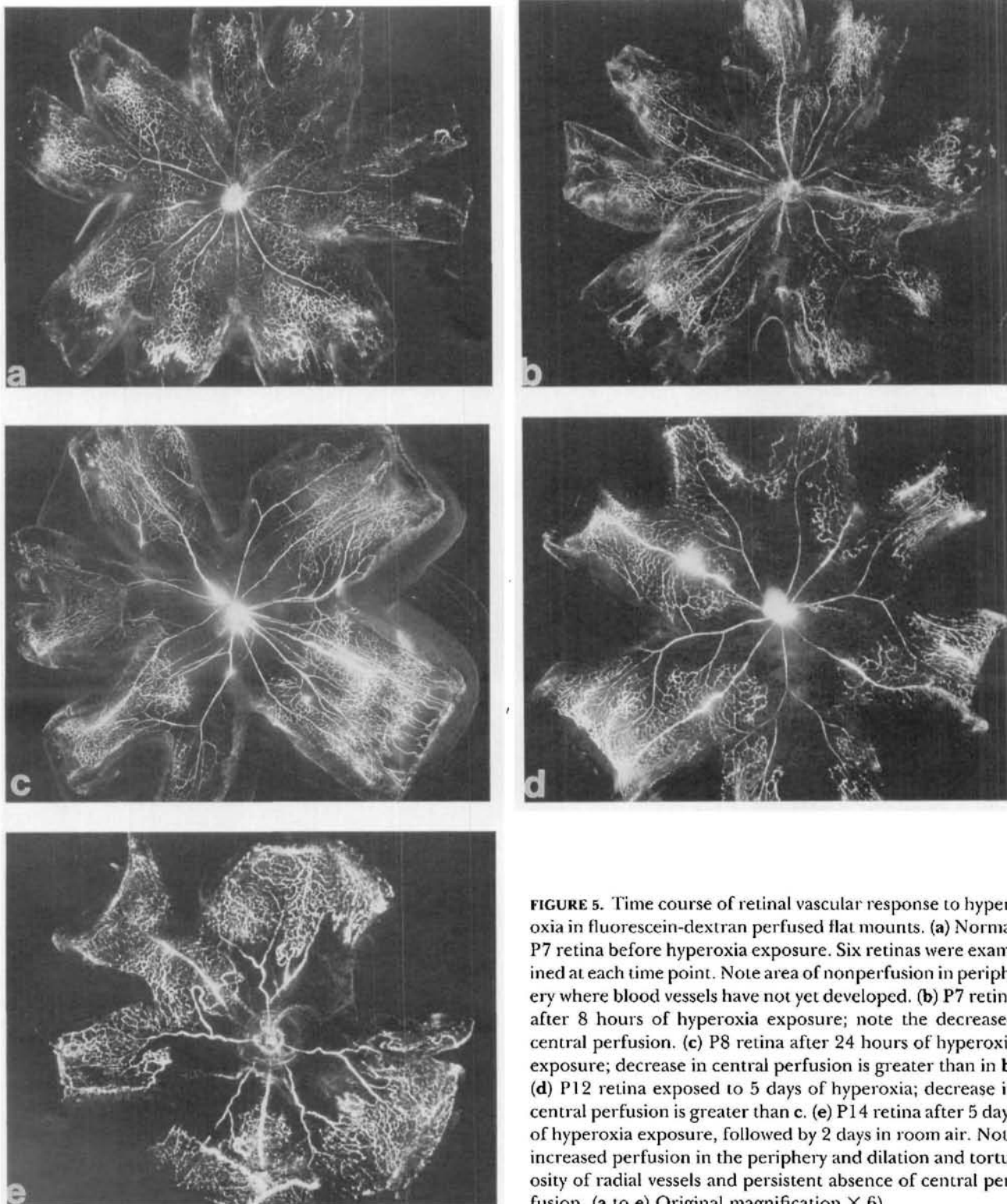


**FIGURE 5.** Time course of retinal vascular response to hyperoxia in fluorescein-dextran perfused flat mounts. (a) Normal P7 retina before hyperoxia exposure. Six retinas were examined at each time point. Note area of nonperfusion in periphery where blood vessels have not yet developed. (b) P7 retina after 8 hours of hyperoxia exposure; note the decreased central perfusion. (c) P8 retina after 24 hours of hyperoxia exposure; decrease in central perfusion is greater than in b. (d) P12 retina exposed to 5 days of hyperoxia; decrease in central perfusion is greater than c. (e) P14 retina after 5 days of hyperoxia exposure, followed by 2 days in room air. Note increased perfusion in the periphery and dilation and tortuosity of radial vessels and persistent absence of central perfusion. (a to e) Original magnification  $\times 6$ .

### GFAP Localization

In the normal mouse retina (Fig. 6a), as previously reported,<sup>15</sup> GFAP was localized in astrocytes whose processes surround the blood vessels in the superficial layer of the retina. The deeper retinal vessels were

surrounded by processes of Müller cells that do not synthesize GFAP (Fig. 6a).<sup>16</sup> After exposure to hyperoxia, there was more intense GFAP staining in astrocyte processes surrounding the vessels of the superficial layer as well as staining of Müller cell processes extending from the internal to the external limiting



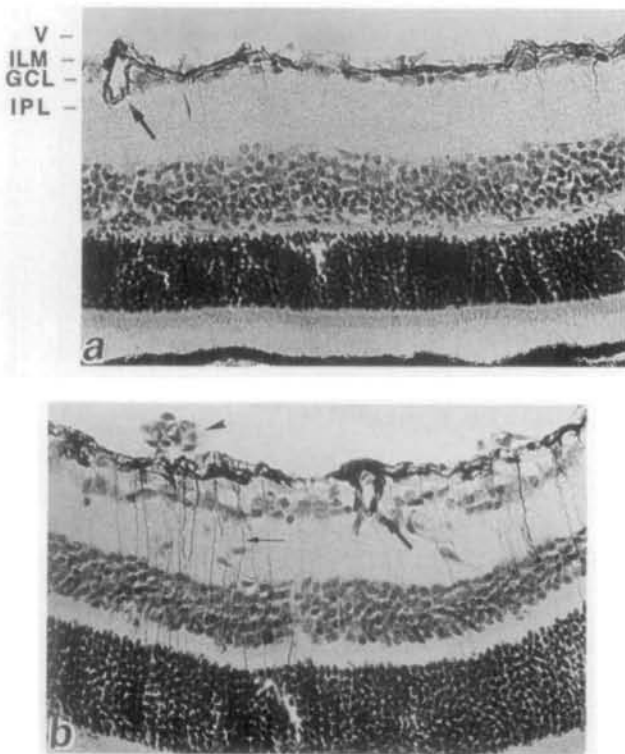


**FIGURE 6.** Glial fibrillary acidic protein (GFAP) immunohistochemistry in 12  $\mu$ m retinal cryosections counterstained with hematoxylin. (a) Normal P17 retina. Note the strong staining of astrocytes in the superficial retina that completely surround the normal superficial vessels (arrow). There is little GFAP immunostaining in the remainder of the retina. (b) Hyperoxia exposed P17 retina. Note the absence of GFAP immunostaining around the neovascular tuft (arrowhead) despite the intense labeling in the adjacent astrocytes and superficial vessels (arrow). Note the GFAP-positive processes of the Müller cells underlying the tuft (thin arrow). (a and b) Original magnification  $\times 90$ . V, vitreous; ILM, internal limiting membrane; GCL, ganglion cell layer; IPL, inner plexiform layer.

membranes (Fig. 6b). GFAP staining in Müller cells tended to be more intense in the regions of retina underlying neovascular tufts. However, the tufts showed no surrounding GFAP immunoreactivity despite their proximity to the superficial vessels and GFAP-positive astrocytes and Müller cell end feet (Fig. 6b).

## DISCUSSION

We have described a reproducible and quantifiable model of oxygen-induced retinopathy in the mouse that will be useful to assess both ROP and other vasoproliferative retinal diseases.

### Murine Retinal Vascular Development

The mouse has a number of characteristics that recommend it as an appropriate species for a model of oxy-

gen-induced proliferative retinopathy. First, the well-described<sup>11,12</sup> normal development of the murine retinal vasculature occurs within 2 weeks of birth, allowing observation of the full spectrum of vascular evolution. Second, the developmental stage of retinal vessels in the newborn mouse retina approximates that of premature infants of 4 to 5 months' gestation.<sup>1</sup> Third, as in the human, this development is initiated by spindle-cell precursors (implicated in the pathogenesis of ROP<sup>17</sup>) that form a superficial layer. This is followed by the development of a deep retinal vascular layer. These characteristics, in conjunction with our quantification method of proliferative retinopathy in cross-section and retinal perfusion assessment method in flat-mount, enabled us to develop a model with proliferative retinopathy suitable for examining neovascularization in ROP.

### Murine Model of Oxygen-Induced Retinopathy: Historical Perspective

In the past, many others have worked with and attempted to develop a mouse model of oxygen-induced proliferative retinopathy with variable success.<sup>1-9,18</sup> Two major problems with the mouse model have been the inconsistency of the neovascular response to hyperoxia and the resultant lack of quantification of that response. The discrepancies among many reports regarding the vasoproliferative response of the neonatal mouse retina to hyperoxia may be attributed in part to differences in such factors as the level, timing, and duration of hyperoxia. In addition, many studies described an oxygen-induced hyaloidopathy as well as retinopathy, leading to further confusion.<sup>19</sup> In the mouse, the hyaloid vasculature, still well-developed at birth, regresses reciprocally as the developing retinal vessels increase in size during normal development.<sup>9,19</sup> Upon exposure to oxygen, the retinal vessels attenuate whereas the interconnected vessels of the hyaloid system and the vitreous become engorged.<sup>4,19,20</sup> Our studies indicate that the developing retinal vessels respond much more consistently to hyperoxia if the hyaloid vessels are more fully regressed, as is the case at P7; the mouse retina then develops a proliferative retinopathy rather than an inconsistent and mixed hyaloidopathy and retinopathy.<sup>1</sup>

### Oxygen-Induced Retinopathy in Mice After Hyaloid Regression

When P7 mice were exposed to hyperoxia, the initial response of the retinal vasculature was initially reversible central vasoconstriction followed by nonperfusion. The more peripheral vessels were spared, perhaps because of persistent interconnected hyaloid remnants maintaining flow. There was often a small avascular zone in the far periphery at the ora serrata where retinal vascular development had not yet oc-

curred (Fig. 5a). After return to room air and before retinal neovascularization at P14, the larger central radial vessels became tortuous and engorged (similar to those seen in plus disease in the human). Neovascularization at the junction between the vascularized and nonvascularized retina then occurred and was followed by regression and normalization of the vascular pattern. We did not attempt to develop cicatricial changes in this mouse model because our goal was to establish a model of retinal neovascularization in ROP that was appropriate for drug testing; cicatricial disease with retinal detachment is irreversible.

We did not observe a large, well-defined, mesenchymal ridge as is seen in human ROP. However, we did observe with light microscopy increased numbers of spindle-shaped cells that created localized thickening of the inner retina at the junction between vascular and avascular retina usually, but not always, in association with proliferative vascular tufts extending above the inner limiting membrane. We could not determine unequivocally that the areas of spindle cell proliferation were associated with arteriovenous shunts. However, the fluorescein-dextran perfused retinas had areas associated with neovascular tufts that appeared to be larger than the corresponding areas stained with RCA lectin I, suggesting that a shunt might be present in the inner retina beneath the tuft.

### Characterization of New Vessels: GFAP Localization

Retinal hemorrhage and other evidence suggest that proliferating vessels in human ROP have a disrupted barrier system and are more permeable than normal retinal vessels.<sup>21</sup> Both astrocytes and Müller cells are important for the formation of the blood-retina barrier.<sup>16,22–25</sup> In this study, the neovascular tufts, unlike the normal vessels in the superficial layer, were not surrounded by GFAP-positive glial processes, suggesting that the newly induced vessels are not associated with astrocytes or Müller cell end feet. Because the glia limitans surrounding these vessels is not intact, they may have a defective blood-brain barrier. Increased leakiness of the proliferative vessels has been seen during India ink retinal perfusion in a feline model of ROP<sup>26</sup>; this defect may be a result of hypoxia-induced degeneration of the astrocytes involved in the formation of the barrier.<sup>27</sup> We did not see an increase in vascular permeability to fluorescein dextran in our material. However, the visualization technique we developed using  $2 \times 10^6$  molecular weight fluorescein-dextran was designed to decrease the degree of penetration of the fluorescein marker through the vessel wall and to maximize visualization of all vessels. In histologic sections through regions of retina near neovascular tufts, we occasionally saw evidence of hemorrhage into the vitreous (see Fig. 2C in Wesolowski and Smith,

page 112 in this issue). Further studies of vascular permeability and of glial-vascular associations in human ROP tissue may provide further insight into the pathology underlying this disease.

Despite the absence of GFAP immunoreactivity surrounding the neovascular tufts, there was an overall increase in GFAP immunoreactivity in the retinas of the oxygen-treated mice. Increased intensity and extent of reactivity were seen along the internal limiting membrane of the retina and appeared to be associated with astrocyte processes. GFAP immunoreactivity was also seen in Müller cell processes. Increases in astrocyte or Müller cell GFAP production as a result of injury, whether caused by trauma,<sup>15</sup> hypoxia/hyperoxia exposure,<sup>28</sup> or degenerative disease<sup>29</sup> has been well documented. It is interesting that the regions of the retina that showed the most intense GFAP staining of Müller cell processes were those regions underlying neovascular tufts. Perhaps this reflects regional variations within the retina in the degree of injury sustained during treatment. The more severely injured regions may then participate in the neovascular response, perhaps by generating increased angiogenic substances or by producing fewer inhibitory factors.

### Quantification of Neovascular Response

Many aspects of oxygen-induced retinopathy, including area of vasoconstriction (in flat-mount), increased intraretinal vascular area, retinal neovascularization, and GFAP immunostaining (in retinal cross-section) might be considered as a means of quantifying and evaluating the response to oxygen. In considering these parameters for quantification, it is important to choose one that minimizes error and makes the model applicable to retinal vasoproliferative diseases other than ROP. Retinal neovascularization extending into the vitreous fits both these criteria.

In this model, neovascularization was observed in all the mice exposed to hyperoxia (but with some variability in the degree of neovascularization, even among littermates (Fig. 3). The method used to quantify retinopathy in this model differs from the grading system of India ink-perfused retinas developed for the kitten by Phelps and Rosenbaum.<sup>30</sup> Counting vascular nuclei in paraffin cross-sections of retinas is more sensitive but also more time consuming than a grading system. Therefore, an angiographic technique such as the fluorescein-dextran method can be used in conjunction with the counting method for rapid screening of retinas (or for an alternative grading system for quantitative evaluation).

The newly developed fluorescein-dextran perfusion technique for delineation of the retinal vasculature in the flat-mounted retina<sup>13</sup> has some advantages over other angiographic techniques, such as India ink perfusion. The technique is rapid, has low background

fluorescence, and delineates the entire retinal vasculature including neovascular tufts. India ink does not consistently perfuse all vessels and does not reproducibly delineate new vessels. On the other hand, fluorescein-dextran is less permanent than India ink because the fluorescein label decays if exposed to excess light. We found the information obtained from flat-mounts of fluorescein-dextran perfused retinas to be complementary to that from paraffin cross-sections. The fluorescein-dextran method reveals the entire vascular pattern at a glance and allows a quick survey of a number of retinas to assess the effect of any intervention on oxygen-induced retinopathy in the mouse model.

In the rat model of ROP, the vaso-obliterative phase has been quantified in India ink flat-mounts.<sup>14</sup> However, the retinal neovascular response does not appear to be as reproducible in the rat as the vaso-obliterative response and graded neovascularization has not been reported.<sup>31,32</sup> Retinal vascular development in the dog is similar to that in the human, and it responds to hyperoxia as it does in the kitten and the mouse with vaso-obliteration and subsequent retinal neovascularization. Flower and Blake<sup>33</sup> also have reported both localized retinal detachments and cicatricial retinal folds in their inbred beagle model. This model could be quantified but, because of the size and expense of the model, it is better suited to qualitative evaluation that can be conducted with a few animals.

The sequence of pathologic events described in this report appears to occur in a number of retinal vasculopathies. In this study, neovascularization was seen after loss of patent vessels in the central retina with hyperoxia exposure. Return to room air from hyperoxia likely caused relative ischemia in the nonperfused retina. Neovascularization at the interface of perfused and nonperfused retina followed. Ischemia, whether from vascular drop-out in diabetes or vein occlusion or vaso-obliteration precipitated by hyperoxia may induce neovascularization by the same mechanism. Agents that inhibit neovascularization in this ROP model could have more general applications in ophthalmology.

## CONCLUSION

We have established a mouse model of oxygen-induced retinopathy that includes reproducible proliferative retinal neovascularization. A fluorescein-dextran perfusion method has been developed to assess the vascular pattern. The proliferative neovascular response has been quantified by counting the vascular nuclei in neovascular tufts extending from the retina into the vitreous. A model of oxygen-induced retinopathy in the mouse with vascular development similar to the human will be useful in assessing medical interven-

tion for ROP and for other proliferative retinal vasculopathies.

## Key Words

retinopathy of prematurity, retinal neovascularization, oxygen-induced retinopathy, fluorescein-dextran angiography, animal model of ROP

## Acknowledgments

The authors thank Erica Wheeler for assistance with GFAP staining, John Kane and Carlene Pavlos for secretarial assistance, David Tompkins for discussions, and David Porter for editorial expertise.

## References

1. Gyllenstein LJ, Hellstrom BE. Experimental approach to the pathogenesis of retrolental fibroplasia: II: The influence of the developmental maturity in oxygen-induced changes in the mouse eye. *Am J Pathol.* 1955;39:475-488.
2. Gole GA, Browning J, Elts SM. The mouse model of oxygen-induced retinopathy: A suitable animal model for angiogenesis research. *Doc Ophthalmol.* 1990;74:163-169.
3. Michaelson IC, Herz N, Lewkowitz E, Kertesz D. Effect of increased oxygen on the development of the retinal vessels. *Br J Ophthalmol.* 1954;38:577-587.
4. Patz A, Eastham A, Higgenbotham DH, Kleck T. Oxygen studies in retrolental fibroplasia: II: The production of the microscopic changes of retrolental fibroplasia in experimental animals. *Am J Ophthalmol.* 1953;36:1511-1522.
5. Ashton N. Retrolental fibroplasia. *Am J Ophthalmol.* 1955;39:153-159.
6. Gyllenstein LJ, Hellstrom BE. Experimental approach to the pathogenesis of retrolental fibroplasia: I: Changes of the eye induced by exposure of newborn mice to concentrated oxygen. *Acta Paediatr Suppl.* 1954;43:131-148.
7. Gyllenstein LJ, Hellstrom BE. Retrolental fibroplasia—animal experiments: The effect of intermittently administered oxygen on the postnatal development of the eyes of full term mice: A preliminary report. *Acta Paediatr.* 1952;41:577-582.
8. Gerschman R, Nadig PW, Snell AC, Nye SW. Effect of high oxygen concentrations on eyes of newborn mice. *Am J Physiol.* 1954;179:115-118.
9. Ashton N. Donders Lecture, 1967: Some aspects of the comparative pathology of oxygen toxicity in the retina. *Br J Ophthalmol.* 1968;52:505-531.
10. D'Amato R, Smith LEH. Microscopic analysis of retinal vessels utilizing fluorescein-labeled high molecular weight dextrans. *Invest Ophthalmol Vis Sci.* 1992;33:1082.
11. Connolly SE, Hores TA, Smith LEH, D'Amore PA. Characterization of vascular development in the mouse retina. *Microvasc Res.* 1988;36:275-290.
12. Blanks JC, Johnson LV. Selective lectin binding of the developing mouse retina. *J Comp Neurol.* 1983;221:31-41.

13. D'Amato R, Wesolowski E, Smith I.E.H. Microscopic visualization of the retina by angiography with high molecular weight fluorescein labeled dextrans in the mouse. *Microvasc Res.* 1993;46:135–142.
14. Penn JS, Gay CA. Computerized digital image analysis of retinal vessel density: Application to normoxic and hyperoxic rearing of the newborn rat. *Exp Eye Res.* 1992;54:329–336.
15. Bignami A, Dahl D. The radial glia of Müller cells in the rat retina and their response to injury: An immunofluorescence study with antibodies to the glial fibrillary acidic (GFA) protein. *Exp Eye Res.* 1979;28:63–69.
16. Hollander H, Makarov F, Dreher Z, van Driel D, Chan-Ling T, Stone J. Structure of the macroglia of the retina: The sharing and division of labor between astrocytes and Müller cells. *J Comp Neurol.* 1991;313:587–603.
17. Kretzer FL, Mehta RS, Johnson AT, Hunter DG, Brown ES, Hittner HM. Vitamin E protects against retinopathy of prematurity through action on spindle cells. *Nature.* 1984;309:793–795.
18. Gole G. Animal models of retinopathy of prematurity. In: Silverman WA, Flynn JT, eds. *Retinopathy of Prematurity*. Boston: Blackwell Scientific; 1985:53–95.
19. Bischoff PM, Wajner SD, Flower RW. Scanning electron microscopic studies of the hyaloid vascular system in newborn mice exposed to O<sub>2</sub> and CO<sub>2</sub>. *Graefes Arch Clin Exp Ophthalmol.* 1983;220:257–63.
20. Patz A. Clinical and experimental studies on retinal neovascularization. *Am J Ophthalmol.* 1982;94:715–743.
21. Flynn JT, O'Grady GE, Herrera J, Kushner BJ, Contolino S, Milam W. Retrolental fibroplasia: I: Clinical observations. *Arch Ophthalmol.* 1977;95:217–223.
22. Janzer RC, Raff MC. Astrocytes induce blood-brain barrier properties in endothelial cells. *Science.* 1987;235:253–257.
23. Risau W, Wolburg H. Development of the blood-brain barrier. *Trends Neurosci.* 1990;13:174–178.
24. Stone J, Dreher Z. Relationship between astrocytes, ganglion cells and vasculature of the retina. *J Comp Neurol.* 1987;255:35–47.
25. Tao-Cheng JH, Brightman MW. Tight junctions of brain endothelium in vivo are enhanced by astroglia. *J Neurosci.* 1988;7:3293–3299.
26. Chan-Ling T, Tout S, Hollander H, Stone J. Vascular changes and their mechanisms in the feline model of retinopathy of prematurity. *Invest Ophthalmol Vis Sci.* 1992;33:2128–2145.
27. Chan-Ling T, Stone J. Degeneration of astrocytes in feline retinopathy of prematurity causes failure of the blood-brain barrier. *Invest Ophthalmol Vis Sci.* 1992;33:2145–2159.
28. Penn JS, Thum LA, Rhem MN, Dell SJ. Effects of oxygen rearing on the electroretinogram and GFAP in the rat. *Invest Ophthalmol Vis Sci.* 1988;29:1623–1630.
29. Eisenfeld AJ, Bunt-Milam AH, Sarthy PV. Müller cell expression of glial fibrillary acidic protein after genetic and experimental photoreceptor degeneration in the rat retina. *Invest Ophthalmol Vis Sci.* 1984;25:1321–1328.
30. Phelps DL, Rosenbaum AL. Effects of marginal hypoxemia on recovery from oxygen-induced retinopathy in the kitten model. *Pediatrics.* 1984;73:1–6.
31. Penn JS, Tolman BL, Lowery LA. Variable oxygen exposure causes preretinal neovascularization in the newborn rat. *Invest Ophthalmol Vis Sci.* 1993;34:576–585.
32. Ricci B, Lepore D, Iossa M, Santo A, D'Urso M, Maggiano N. Effect of light on oxygen-induced retinopathy in the rat model. *Doc Ophthalmol.* 1990;74:287–301.
33. Flower RW, Patz A. Oxygen studies in retrolental fibroplasia: IX: The effects of elevated arterial oxygen tension on retinal vascular dynamics in the kitten. *Arch Ophthalmol.* 1971;85:197–203.